JOURNAL OF COMPUTATIONAL PHYSICS 78, 160–177 (1988)

Staggered and Nonstaggered Grids with Variable Node Spacing and Local Time Stepping for the Random Choice Method

JAMES J. GOTTLIEB

Institute for Aerospace Studies, University of Toronto
4925 Dufferin Street, Downsview, Ontario, Canada M3H5T6

Received April 30, 1987; revised September 4, 1987

The staggered grid and random sampling procedure used currently in the random choice method for solving hyperbolic equations like those for one-dimensional unsteady flows and two-dimensional axisymmetric and planar steady supersonic flows are reviewed and extended to include variable node spacing. A nonstaggered grid with variable node spacing, more convenient random sampling process, and local time stepping are then introduced, and there use in significantly reducing computational time and costs in solving certain problems is discussed. These methods are easily applied in the random choice method for problems with more dimensions. © 1988 Academic Press, Inc.

1. INTRODUCTION

The random choice method (RCM) was developed to solve nonlinear hyperbolic partial differential equations and has been used successfully in solving gas-dynamic problems such as one-dimensional unsteady flows and two-dimensional planar and axisymmetric steady supersonic flows. This is essentially a finite-volume method, and it is explicit in that it solves a Riemann problem in each cell at one time level and then uses random sampling to assign or advance the solution to the next time level. The main advantages of the RCM are its simplicity and its ability to resolve discontinuities exactly without numerical dispersion or dissipation, without overshoots and undershoots, and without any special procedures for capturing discontinuities.

A precusor to the RCM is the finite-difference scheme of Godunov [1]. He introduced the use of Riemann problems to computational fluid dynamics, but used a deterministic integration procedure for the assignment of mass averaged solutions to the next time level. Glimm [2] kept the Riemann problems in his invention of the RCM but introduced random sampling to replace the averaging procedure and thereby conserve mass, momentum, and energy. He applied the method as a theoretical tool to obtain existence proofs for all time for weak solutions of hyperbolic systems of conservation laws. Glimm's work is a theoretical milestone, even though the convergence rate of his original RCM with sampling by means of pseudo-random numbers is too slow for practical numerical computations (node

0021-9991/88 $3.00

spacing is unfavorably small). The RCM was made into a practical numerical method by Chorin [3, 4], who introduced quasirandom numbers into the sampling process and the use of one random number per time step, in order to increase the convergence rate (or permit larger node spacings). The RCM was also improved by Sod [5], Collella [6], and others, and since the late 1970s it has been employed successfully to solve many problems in gas dynamics (e.g., [7–15]).

In these past studies a staggered grid with a uniform node spacing has normally been used in the RCM (Fig. 1), with few exceptions [6, 16, 17]. In fact, a lot of the past work implicitly suggests that a staggered grid is the best and most natural choice, and newcomers to the RCM adopt this type of grid without question. The primary purpose of the present paper is to introduce a more useful nonstaggered grid with both variable node spacing and local time stepping. Local time stepping means that solutions for individual cells of different width advance in time by steps which are effectively controlled by their own Courant–Fredrichs–Lewy (CFL) criterion. A technically different but equivalent quasirandom sampling procedure is also introduced because it is simplifies computer program logic and helps make local time stepping easy to apply. These new techniques are superior to the past method of employing a staggered grid with a fixed node spacing which is everywhere small with cell solutions all advancing by the small time step. The significant savings in computational solution time and cost are illustrated with selected problems. The nonstaggered grid with variable node spacing and local time stepping for the RCM can also be applied to multidimensional problems such as unsteady flows in two and three dimensions, and computational savings for such problems should be even more significant.

In this paper the case of one-dimensional unsteady gas flows is used to illustrate many concepts and results. However, these same concepts will apply virtually directly to other problems involving nonlinear hyperbolic equations with two independent variables (e.g., two-dimensional planar and axisymmetric steady supersonic flows, longitudinal stress wave motion in long or thin viscoelastic rods).

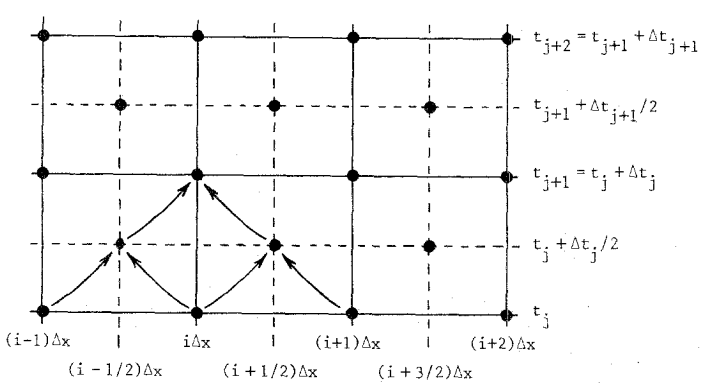

FIG. 1. Staggered grid for the case of one-dimensional unsteady flows.

2. Staggered Grid and Quasirandom Sampling

As in most explicit numerical schemes, the RCM integrates the hyperbolic conservation equations by computing the solution at a new time level by using the solution from the old time level. A staggered grid generally employed to solve one-dimensional unsteady flow problems with the RCM is shown in Fig. 1. The spacing Δx between adjacent grid nodes at each time is constant. The jth time step Δt_j between time levels t_j and $t_j + \Delta t_j$ actually consists of two time steps, each of equal size $\Delta t_j/2$. For example, the first half-step uses known solutions at nodes $i\,\Delta x$ and $(i+1)\,\Delta x$ at time level t_j to find the solution at the intermediate or staggered node $(i+1/2)\,\Delta x$ at the next time level $t_j + \Delta t_j/2$. The second half-step is used to get the solutions at level t_{j+1}, back at the original node locations (e.g., $i\,\Delta x$), as indicated by arrows on the diagram. Note that each half-step in time is restricted by the CFL time step criterion for computational accuracy and/or stability. This time increment is normally determined for the first half-step and then simply held constant for the second half-step, mainly to reduce computational effort of recomputing the new time step. Boundary conditions also have to be applied at the left- and right-hand sides of the grid, in the same manner as for a nonstaggered grid, and these will be discussed later.

The solution at a half-step is related to the previous half-step by the solution of a series of Riemann or initial value problems, and in the RCM these solutions are sampled for each cell in the computational field to advance to the next time level. The Riemann problem for one cell is normally written as

$$U(x, t_j) = \begin{cases} U(x_i, t_j) & \text{if} \quad x < (i+\tfrac{1}{2})\,\Delta x, \\ U(x_{i+1}, t_j) & \text{if} \quad x \geqslant (i+\tfrac{1}{2})\,\Delta x, \end{cases} \tag{1}$$

where $U(x_i, t_j)$ and $U(x_{i+1}, t_j)$ are known initial data at the nodes (x_i, t_j) and (x_{i+1}, t_j). Hence, the initial data $U(x, t_j)$ is piecewise constant; it equals either $U(x_i, t_j)$ or $U(x_{i+1}, t_j)$ and contains a discontinuity at the cell center. With increasing time beyond t_j this discontinuity will break into leftward and rightward moving waves that are separated by a contact surface. Each wave can be either a shock or a rarefaction wave, and this results in four possible wase patterns that are self-similar (i.e., depend on x/t only), as shown in Fig. 2. (A special fifth case of two rarefaction waves and two contact surfaces separated by a vacuum is not considered.) For a specific set of initial conditions given by $U(x_i, t_j)$ and $U(x_{i+1}, t_j)$, the solution of the Riemann problem for the resulting wave pattern and wave strengths can be determined by some convenient iterative procedure. However, Riemann solvers [1, 3–6, 12–14] are neither needed nor presented in this paper.

Once the wave pattern, wave strengths, and flow properties in each zone between the waves and contact surface are known, random ampling may be applied to choose and assign a solution to the intermediate or staggered node for the next time level. A random number Ω in the range from 0 to 1 is chosen from a uniform probability density distribution, and a point q at time level $t_j + \Delta t_j/2$ (shown as a

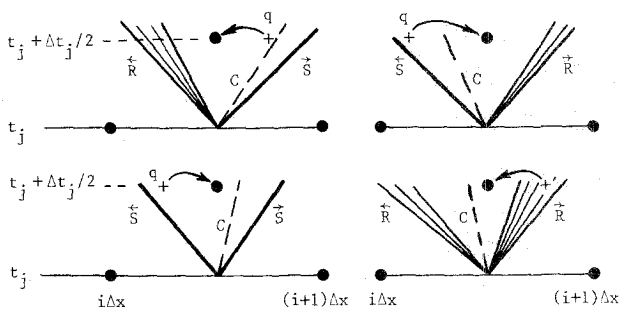

FIG. 2. Four possible wave patterns in the solution of a Riemann problem, showing shock (S) and rarefaction (R) waves separated by a contact surface (C).

cross in Fig. 2) is located according to $x_q = (i + \Omega)\,\Delta x$. The chosen solution from point q in the wave pattern is then assigned to the intermediate node at time level $t_j + \Delta t_j/2$.

Now consider this random sampling in more detail, for staggered grids of uniform node spacing for which the node at the next time level is located at the center of the cell and also off-center. The range for point q at which the wave pattern is sampled at the new time level $t_j + \Delta t_j/2$ is illustrated in Fig. 3. In Fig. 3a the assignment node is at the center of the cell at the location $(i + 1/2)\,\Delta x$, and the sampling point q located at $x_q = (i + \Omega)\,\Delta x$ varies linearly from the left side of the cell ($\Omega = 0$), through the center of the cell ($\Omega = \frac{1}{2}$), and over to the right side of the cell ($\Omega = 1$). The width of the sampling point range is equal to the constant node spacing separation (Δx).

In Fig. 3b the assignment node is off-center at the location $(i + \lambda)\,\Delta x$, where

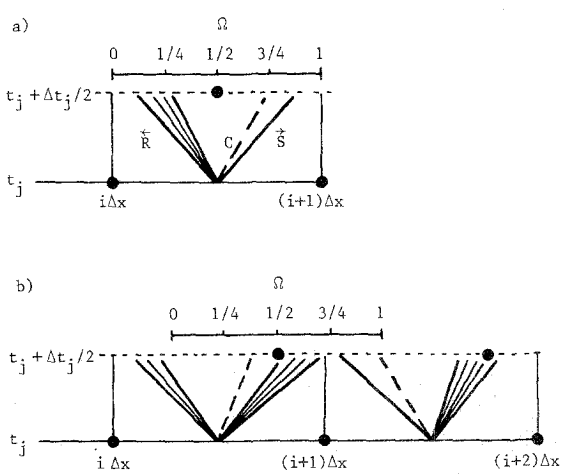

FIG. 3. Random sampling for the cases of an assignment node in the cell center (a) and off-center (b).

$0 \leqslant \lambda \leqslant 1$. The sampling point q located at $x_q = (i + \lambda - \frac{1}{2} + \Omega)\,\Delta x$ takes the linear range from $(i + \lambda - \frac{1}{2})\,\Delta x$ to $(i + \lambda + \frac{1}{2})\,\Delta x$, which again has a width equal to the constant node spacing Δx. However, the random sampling is no longer confined to only one cell which contains the assignment node at $(i + \lambda)\,\Delta x$, as shown in Fig. 3b, but also includes an adjacent cell on the left ($\lambda < \frac{1}{2}$) or right ($\lambda \geqslant \frac{1}{2}$). In this case the random sampling covers the parts of two separate wave patterns from adjacent cells, and these patterns are the solutions of two different Riemann problems. If λ is equal to either 0 or 1 for the case of a nonstaggered grid the random sampling will then span abutting halves of two adjacent cells, and exactly half of each wave pattern will be sampled [16].

Now consider the most general case when a grid has staggered nodes that are nonuniformly spaced. Let the minimum separation between two adjacent nodes be denoted by Δx_m, and let the CFL criterion dictate the time step Δt according to $\Delta x_m/(2W_{\max})$, where $W_{\max}$ is the maximum value of $|u| + a$ for all nodes. Let the cell of interest which contains the assignment node have a width Δx, and let the cells on the immediate left and right sides have different widths denoted by Δx_a and Δx_b, respectively, as depicted in Fig. 4. Let the assignment node be located at a dis-

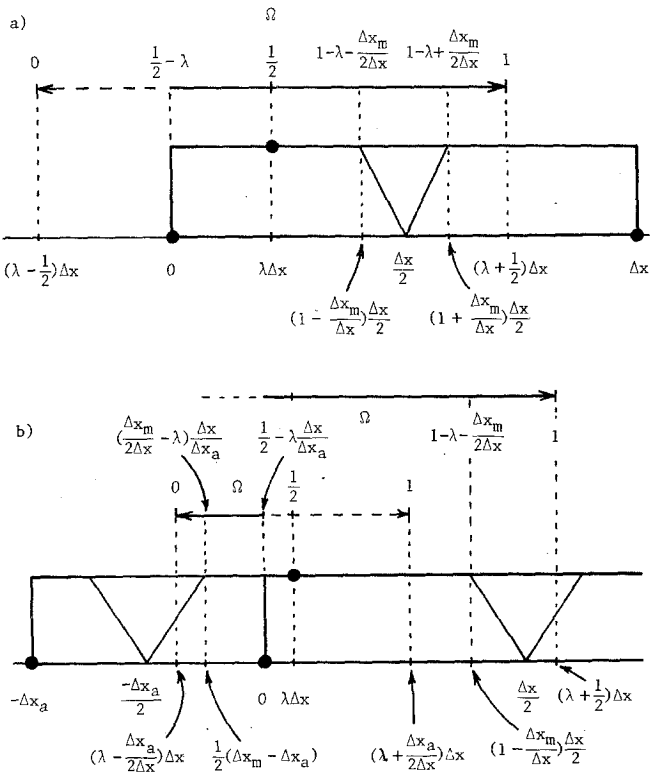

FIG. 4. Random sampling for cases A and B when the assignment node is well inside the left part of the cell (a) and near the near the left boundary (b).

tance $\lambda\,\Delta x$ inside the center cell of width Δx, at the next time level, where $0 \leqslant \lambda \leqslant 1$. In this general case the random sampling is much more complex than that encountered for a uniform node spacing, because the width of the sampling range is not obvious and the sampling in this range is no longer linear across abutting cells. In the present approach the random sampling is subdivided into three cases for clarity.

In the first case (A) the assignment node lies well inside the cell of width Δx such that $\Delta x_m/2\,\Delta x \leqslant \lambda \leqslant 1 - \Delta x_m/2\,\Delta x$. The random sampling will include all of the wave pattern inside this cell, but the stretched or reduced sampling range outside the cell will be too short to overlap the patterns in the cells on the immediate left and right sides. This case is illustrated in Fig. 4a, for the case of $\lambda < \frac{1}{2}$. For random numbers in the range $0 \leqslant \Omega < \frac{1}{2} - \lambda$ the sampling does not overlap the pattern in the cell on the left, and the state for the node at $x = 0$ is then assigned to the node at $x = \lambda\,\Delta x$ (for the next time level). The same assignment occurs if $\frac{1}{2} - \lambda \leqslant \Omega \leqslant 1 - \lambda - \Delta x_m/2\,\Delta x$, because the wave pattern in the center cell is not sampled. On the other hand, the state at the node at $x = \Delta x$ is assigned to the node at $x = \lambda\,\Delta x$ if $1 - \lambda + \Delta x_m/2\,\Delta x \leqslant \Omega \leqslant 1$. Consequently, the pattern within the cell of width Δx is sampled and assigned to the node at $x = \lambda\,\Delta x$ only if the random numbers lie within the range $1 - \lambda - \Delta x_m/2\,\Delta x < \Omega < 1 - \lambda + \Delta x_m/2\,\Delta x$. The Riemann problem need only be computed if the pattern is actually going to be sampled.

When $\lambda \geqslant \frac{1}{2}$ for case A the sampling range is shifted to the right. The random sampling now occurs entirely within the center cell if $0 \leqslant \Omega \leqslant 3/2 - \lambda$, and the pattern in this cell is sampled only if $1 - \lambda - \Delta x_m/2\,\Delta x < \Omega < 1 - \lambda + \Delta x_m/2\,\Delta x$. Because this is a mirror image of the previous case of $\lambda < \frac{1}{2}$, the additional details are easy to construct and thus omitted.

In the second case (B) the assignment node lies sufficiently near to the left side of the center cell of width Δx such that $\lambda < \Delta x_m/2\,\Delta x$. The random sampling can now include data from a part of the wave pattern in the left cell as well as data from a part of the wave pattern from the center cell, depending on the value of the random number, as illustrated in Fig. 4b. For the random numbers $0 \leqslant \Omega < (\Delta x_m/2\,\Delta x - \lambda)\,\Delta x/\Delta x_a$ a right part of the wave pattern in the left cell is sampled, whereas for the random numbers $1 - \lambda - \Delta x_m/2\,\Delta x < \Omega < 1$ more than half of the left side of the wave pattern in the center cell will be sampled. For the remainder of the random numbers $(\Delta x_m/2\,\Delta x - \lambda)\,\Delta x/\Delta x_a \leqslant \lambda \leqslant 1 - \lambda - \Delta x_m/2\,\Delta x$ the state for the node $x = 0$ is assigned to the node at $x = \lambda\,\Delta x$ (for the next time level). Note that the random sampling in the left and center cells are done with different scales, as depicted in Fig. 4b. The scale for the center cell is the same as that shown in Fig. 4a, and the scale for the left cell is different by the factor $\Delta x_a/\Delta x$.

In last case (C) the assignment node lies sufficiently near to the right side of the center cell such that $\lambda > 1 - \Delta x_m/2\,\Delta x$, and the wave pattern in the right cell may be sampled. This is essentially a mirror image of case B, and the details are therefore omitted.

A few comments regarding these results are worthwhile. First, the random sampling for the staggered grid with nonuniform node spacing is fairly complex compared to that for uniform node spacing, and a naive straightforward approach

of linearly sampling across both cells would be incorrect. Second, the results for the staggered grid with a nonuniform node spacing will reduce to the earlier results for a staggered or nonstaggered grid with a uniform node spacing. Third, a staggered grid constructed of an adjoining fine and coarse node spacing will always have a node off-center at alternate time levels at the fine and coarse mesh juction. For this peculiar cell with the off-centered node at the next time level only case A is actually needed in the random sampling process. Finally, the random sampling for the general case which involves cases A, B, and C gives the RCM the capability for adaptive gridding. Nodes at new time levels may not only be increased or decreased but may also be placed at any given spatial locations, although suitable algorithms for automatically allocating and positioning nodes would be required.

Before leaving this section it is worth mentioning that the random sampling in the RCM is really a Monte Carlo integration process; it is not a Monte Carlo simulation of a purely random process. Consequently, quasirandom numbers instead of pseudorandom numbers may (or should be) incorporated to accelerate the convergence rate or improve the numerical accuracy for a given node spacing [6, 18, 19] (for which the error is of order $\Delta x\,|\ln\{\Delta x\}|$ in contrast to $\Delta x^{1/2}$ for pseudo-random numbers). The best possible quasirandom numbers for the RCM are presently those of Van der Corput [19, 20], because they are well equidistributed. In order to preserve this improved convergence rate or accuracy in the quasi-Monte Carlo integration process, only one quasirandom number is used for all Riemann problems at one time level [3].

3. Alternate Quasirandom Sampling Procedure

An equivalent but technically different quasirandom sampling procedure is now described for a staggered grid with either uniform or nonuniform node spacing. As with the previous sampling technique, at any time level the flow field may be represented discretely by the flow properties at a finite number of grid nodes. However, in the construction of the Riemann problem between two nodes with initial data (e.g. $i\,\Delta x$ an $(i+1)\,\Delta x$), the actual position of the discontinuity or mismatch in the constant states $U(x_i, t_j)$ and $U(x_{i+1}, t_j)$ may be considered unknown. In order to insert this discontinuity, one may assume that it has an equal chance or probability of occurring in each subinterval of the cell length Δx. The Riemann problem may then be expressed as

$$U(x, t_j) = \begin{cases} U(x_i, t_j) & \text{if } x < (i+\Omega)\,\Delta x, \\ U(x_{i+1}, t_j) & \text{if } x \geqslant (i+\Omega)\,\Delta x, \end{cases} \tag{2}$$

where Ω is a quasirandom number in the range from 0 to 1 (chosen from a uniform probability density distribution). For a particular set of initial conditions given by $U(x_i, t_j)$ and $U(x_{i+1}, t_j)$, the Riemann problem may be solved to obtain the type of wave pattern, wave strengths, and flow properties in each region between the waves

and contact surface, and this pattern can then be mapped onto a time-distance diagram, as illustrated in Fig. 5. Now, instead of sampling the wave pattern solution and assigning it to the node at the next time level, the solution of whatever part of the wave pattern that overlaps the staggered grid node at the next time level is assigned directly to this node. This node may be located exactly at the cell center for a perfectly staggered grid, as depicted in the left pattern, or it can be located more generally anywhere in this cell at this time level, as indicated in the right pattern.

If the assignment node is located in the center of the cell ($\lambda = \frac{1}{2}$), then the wave patterns in the cells on the immediate left and right sides of this center cell cannot overlap this node, because the CFL time step criterion is obeyed. Therefore, for $0 \leqslant \Omega \leqslant 1$ the wave pattern for this cell will be the only one sampled. If the assignment node is off-center then the pattern from the cell on the left side may overlap this node ($\lambda < \frac{1}{2}$, $\Omega > \lambda + \frac{1}{2}$), or conversely the pattern from the cell on the right side may overlap this node ($\lambda > \frac{1}{2}$, $\Omega < \lambda - \frac{1}{2}$). These results correspond to the simplest case of a uniform node spacing.

The extension of the alternate sampling procedure to the case of a grid with a nonuniform node spacing is rather easy, in contrast to the corresponding extension in the last section. If the assignment node lies well inside of the center cell of width Δx such that $\Delta x_m/2\,\Delta x \leqslant \lambda \leqslant 1 - \Delta x_m/2\,\Delta x$, which corresponds to case A of the previous section, then the assignment can come only from the pattern within this cell. Furthermore, the pattern is sampled only if $\lambda - \Delta x_m/2\,\Delta x < \Omega < \lambda + \Delta x/2\,\Delta x$. For case B for which $\lambda < \Delta x_m/2\,\Delta x$ the assignment node lies sufficiently close to the left side of the center cell such that the assignment may come from the wave pattern in the left or center cell. The assignment is from the left cell if $1 - \Delta x_m/2\,\Delta x_a + \lambda\Delta/\Delta x_a < \Omega < 1$, and from the center cell if $0 < \Omega < \lambda + \Delta x_m/2\,\Delta x$. For case C with $\lambda > 1 - \Delta x_m/2\,\Delta x$ the assignment is similar to that for case B, and the details are omitted.

The previous and alternate random sampling procedures are not only similar but equivalent; in the previous method the wave pattern is fixed at the cell center at one time level and the sampling point is moved randomly at the next time level, whereas in the alternate approach the pattern is moved randomly while the assignment node is fixed. However, the alternate sampling procedure is easier to implement in computer programs (significantly fewer logic and assignment statements and reduced computational effort), especially in the case of a staggered grid with variable node spacing.

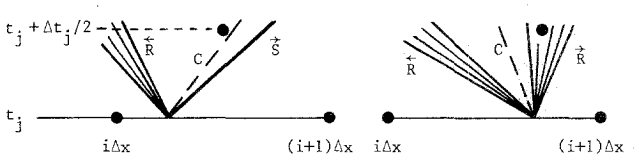

FIG. 5. Alternate random sampling in which the wave pattern is moved randomly within the cell.

Let the locations of the assignment node and discontinuity be given by $(i+\beta)\,\Delta x$ and $(i-\Omega)\,\Delta x$, respectively, where β normally has values between 0 and 1. A reference velocity V may then be defined as the distance between these two locations divided by a half-step denoted by Δt, and it will simply be equal to $(\beta-\Omega)\,\Delta x/\Delta t$. A solution assignment for the pattern on the left side of Fig. 5 would proceed as follows. If V is larger than the rightward moving shock, then the state $U(x_{i+1}, t_j)$ would be assigned at the next level to the node located in front of this shock. If V lies between the velocities of the contact surface and the tail of the leftward moving rarefaction wave, then the state between the contact surface and tail would be assigned to the node which must also lie between the contact surface and tail, as shown in the diagram, and so on and so forth for sampling. This helps illustrate the simplicity of both the random sampling and assignment of states to nodes in this alternative approach.

4. Nonstaggered Grid and Quasirandom Sampling

A nonstaggered grid for solving one-dimensional unsteady flow problems is depicted in Fig. 6. The entire grid width from x_1 to x_m is shown, where m denotes the total number of nodes for the numerical grid, but only six time levels from t_1 to t_6 are needed for illustration. The spacing between adjacent nodes can be constant as indicated or variable, and the time steps between successive levels are also limited by the CFL criterion (based on the smallest cell width).

The use of this nonstaggered grid in the RCM is now explained. Since t_1 is the initial or first time step in the numerical computations, the first step is to specify the states $U(x_i, t_1)$ for all interior nodes $(i=2, 3, ..., m-1)$. One quasirandom number is now selected for this entire time level t_1, and let this number Ω lie between $\frac{1}{2}$ and 1. This then places the discontinuities at $x_i+\Omega(x_{i+1}-x_i)$, in the right half of each cell for time level t_1.

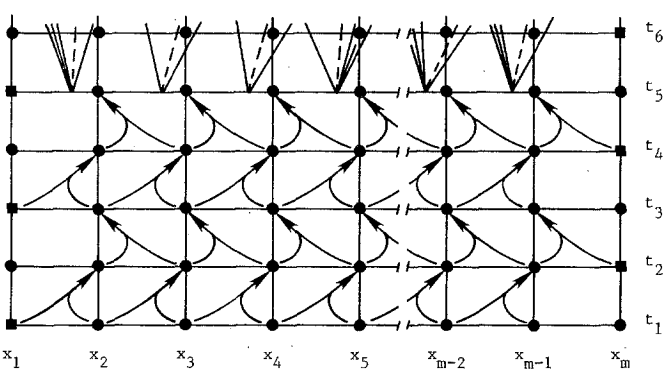

FIG. 6. Nonstaggered grid with sampling procedure shown, for the case of one-dimensional unsteady flows

Then a boundary condition for a closed, open, or nonreflecting grid end needs to be applied at the left side of the grid (when $\Omega \geq \frac{1}{2}$), along with the known state

because this state is not required at time level t_1. The next step is to apply the CFL time step criterion to obtain $\Delta t_1 = t_{j+1} - t_j$, by using the states $U(x_i, t_1)$ for which $i = 1, 2, ..., m-1$. Note that this time step is obtained after the boundary conditions are applied, so that this boundary state is properly included in determining the time step.

The next step is to compute Riemann solutions for all cells, except for the last one on the right side (not required), and then map the resulting wave patterns on a time-distance diagram (as illustrated between levels t_5 and t_6). These patterns will overlap the nodes on the right side of the cell at level t_2 (or almost overlap this node), as illustrated in Fig 6, because Ω lies between $\frac{1}{2}$ and 1. Note that these patterns cannot overlap the left node of the cells because the CFL criterion sufficiently limits the time step.

The reference velocity V_i is given by $(\beta - \Omega)(x_{i+1} - x_i)/\Delta t_1$, for which β is unity for an assignment to the right node at level t_2. (V_i is constant for all cells only if the node spacing is uniform.) By using this reference velocity and the assignment procedure explained previously, the proper states will then be assigned to the right-hand nodes of the cells at level t_2.

This process may be repeated to advance the solution to time level t_3, with a few subtle changes. A second quasirandom number Ω is selected, and it is now assumed to have a value between 0 and $\frac{1}{2}$. This then places the discontinuities in the left half of each cell. The boundary condition is now applied to the right side of the grid (when $\Omega < \frac{1}{2}$), with state $U(x_{m-1}, t_2)$, in order to determine the state $U(x_m, t_2)$ at the outermost right node. The CFL criterion is then used to get the time step Δt_2, by using the states $U(x_i, t_2)$ for which $i = 2, 3, ..., m$. Following this step is the computations of the Riemann problems for all cells except the first one on the left side (not required), and a mapping of the wave patterns on a time-distance diagram. Since Ω lies between 0 and $\frac{1}{2}$ the patterns will in general overlap nodes on the left side of the cells at time level t_3. With $V_i = (\beta - \Omega)(x_{i+1} - x_i)/\Delta t_2$ and β equal to zero for an assignment to the left node, the proper states may be assigned to the nodes at level t_3.

The solutions can be advanced to subsequent time levels by continuing this straightforward procedure. If solution assignments are made to the right (for $\Omega \geq \frac{1}{2}$), then the bounary conditions are applied at the left side of the grid, and conversely. The outermost nodes at which boundary conditions need to be applied are shown as squares in Fig. 6. Note that Riemann solutions should not be assigned to any boundary nodes (e.g., squares), because the states at such nodes are dictated by boundary conditions, and these will be wasted when the boundary conditions are subsequently applied.

Sequential quasirandom numbers from the Van der Corput sequence always oscillate from values above $\frac{1}{2}$ to values below $\frac{1}{2}$. Hence, the direction of the

assignement of successive sets of states of Riemann problems from one time level to the next also oscillates from right to left. This is illustrated in Fig. 6 (by the wavy lines with arrow heads). Pseudorandom numbers and some quasirandom numbers other than Van der Corput's sequence would not produce such a regular assignment oscillation or flip-flop. However, this would not invalidate the new sampling and assignment procedure for the case of the nonstaggered grid, but these other random number sequences would have a poorer convergence rate, unless they were better sequences than that of Van der Corput.

5. Variable Node Spacing and Local Time Stepping

In many computational problems the flow in a localized part of the grid has high gradients and elsewhere they are substantially less. One example is the case of a spherical explosion with higher flow gradients nearer the origin, and another is an unsteady flow along a duct with a local reduction in area (of finite length) where the flow gradients are relatively large. A fine grid with closely spaced nodes is required to accurately resolve the flow properties where their gradients are large, whereas a coarse grid would provide sufficient (equivalent) accuracy elsewhere. The primary advantage of using variable node spacing with a fine grid in parts of the flow and a coarse grid elsewhere is the reduction in the total number of cells and the corresponding reduction in the computational effort and costs (compared to the case of using the fine grid throughout the flow field). For example, if the number of cells for a problem with a combined fine and coarse grid could be reduced by a factor of three, then the CPU time would be diminished by about a factor of three, because the time steps would be nearly the same, since the CFL criterion would be based on the fine grid. Furthermore, if the computations could proceed for the small cells at their CFL dictated time step and for the larger cells at their CFL dictated time step, then this local time stepping would further reduce computational effort. This is possible in the RCM with a variable grid.

For the case of a nonstaggered grid with a variable node spacing let the cell of interest have a width Δx and let the minimum node spacing be Δx_m. In the last section we have already seen how the wave patterns were sampled and the solutions assigned to the nodes at the next time step. Now we will look more closely at certain aspects of random sampling within cells to help illustrate how local time stepping may be implemented. Two cells of width Δx_m and Δx are shown in Fig. 7, with a wave pattern included. In the case of the smaller cell the time stepping always will proceed with the step $\Delta t = \Delta x_m / W_{\max}$ from the CFL criterion. The wave pattern might overlap either the left node ($\Omega < \frac{1}{2}$) or right node ($\Omega \geqslant \frac{1}{2}$), as explained earlier. In this case the Riemann problem will have to be solved for every time step.

In the case of the larger cell shown in Fig. 7 the wave pattern will not overlap either the left or right nodes if the random number has values in the range $\Delta x_m / 2\,\Delta x < \Omega < 1 - \Delta x_m / 2\,\Delta x$. In this case there is no need to solve the Riemann

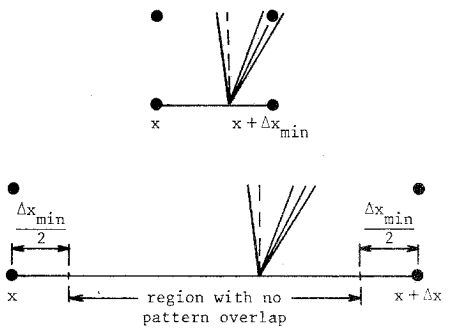

FIG. 7. Region of no wave pattern overlap with nodes at the next time level in a large cell having a width Δx (larger than the smallest cell of width $\Delta x_{\min}$).

problem because it will not be sampled, and this work can simply be skipped. There is also no need to do any state assignment, since the state at this node does not change from the old to the new time level. The Riemann problem, random sampling and state assignment will only have to be done in the proportion $\Delta x_m/\Delta x$ of the time steps for this larger cell, because this is the ratio of the time the random number falls in the intervals $0 \leqslant \Omega \leqslant \Delta x_m/2\,\Delta x$ and $1 - \Delta x_m/2\,\Delta x \leqslant \Omega \leqslant 1$. This means that the Riemann problem, sampling, and state assignment for the larger cell are effectively being done at time intervals equal to $(\Delta x/\Delta x_m)\,\Delta t$, on the average, which is essentially the CFL criterion for the larger cell.

This is illustrated in Fig. 8, where the numerical grid is constructed of cells of minimum width Δx_m on the left and cells of larger width $3\,\Delta x_m$ on the right. The Riemann problem, sampling, and state assignement are done for cells with wave patterns shown are solid lines, whereas those that are skipped appear as dashed lines. The state at node x_{i-1} is updated every time level, whereas the node at x_{i+1} is updated at time levels t_{j+1}, t_{j+4}, and t_{j+7}. Note that this updating is not always this regular, but depends on the random number sequence.

The technique of skipping over needless Riemann problems, sampling, and state

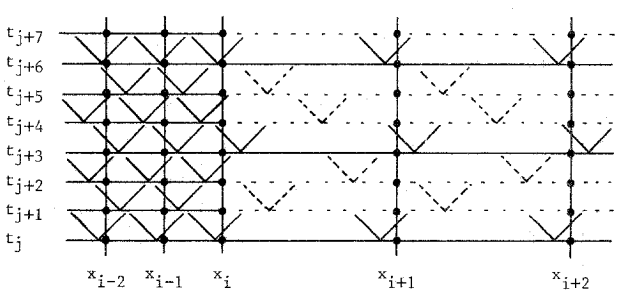

FIG. 8. Illustration of local time stepping for a grid with a fine node spacing Δx_m on the left and a coarse node spacing of $3\,\Delta x_m$ on the right.

assignments is nothing less than the process of local time stepping. The remarkable advantages of this local time stepping in the RCM for a nonstaggered grid with variable node spacing is that it is trivial to implement, does not involve any type of approximation, and does not reduce the quality of the numerical results.

In the solution of hyperbolic equations in weakly conservative form (includes source terms) by the RCM, the solution proceeds in two stages. The Riemann problem for the homogeneous equations is solved first, random sampled, and the solution assigned to the appropriate node. For the unsteady gas-dynamic equations this corresponds to the solution of $U_t + f(U)_x = h(U, x)$ with the source terms $h(U, x)$ simply ommitted, where $U = [\rho, \rho u, p/(\gamma - 1) + \rho u^2/2]$ and $f(U) = [\rho u,\ p + \rho u^2,\ \gamma p u/(\gamma - 1) + \rho u^3/2]$. Then this intermediate solution $\tilde{U}$ is corrected by means of an operator splitting technique (time splitting) first introduced to the RCM by Sod [5]. This step takes the form $U_t = h(\tilde{U}, x)$, where $h(U, x) = -\beta[\rho u,\ \rho u^2,\ \gamma p u^3/2]$ for an area change with $\beta = (1/A)\, dA/dx$. The final results of a first-order finite-difference correction may be written explicitly as $\rho = \tilde{\rho}(1 - \beta\tilde{u}\, \Delta t)$, $u = \tilde{u}$, and $p = \tilde{p}(1 - \beta\gamma\tilde{u}\, \Delta t)$. The question here is whether such operator-splitting corrections can also be skipped along with the Riemann problems for coarse parts of the grid, in order to save additional computational effort. Although this is not necessarily recommended, it can be achieved if certain precautions are taken. One approach is now described.

Consider what happens to the state at one node with time. For the node at location x_{i+1} in Fig. 8 the state is known at the initial time level t_j. This state is altered at time t_{j+1} by the assignment from the Riemann problem, and this happens again at time t_{j+4}. In between the only changes are due to operator splitting. If it was done at each intermediate time steps the updated variables at time t_{j+3} may be written as $\rho_{j+3} = \tilde{\rho}_{j+1}[1 - \beta\tilde{u}_{j+1}(t_{j+3} - t_j)] + O(\Delta t)$, $u_{j+3} = \tilde{u}_{j+1}$, and $p_{j+3} = \tilde{p}_{j+1}[1 - \beta\gamma\tilde{u}_{j+1}(t_{j+3} - t_j)] + O(\Delta t)$. If these corrections were done in one time step only, they would be very similar but not have the higher order terms. Hence, to first order the corrections can be done at each intermediate time level or all at once at some appropriate later time level.

If intermediate corrections are skipped, then the correction taken later must be done for a larger time interval that includes all previous time levels that were skipped. In addition, this correction should be made to all states at nodes on the time level at which the Riemann problem needs to be solved for the cells on either side of this node, and the correction should be done before the Riemann problem is solved. Such considerations make skipping intermediate corrections fairly tedious.

Before leaving this section it is worthwhile to note that waves moving from fine to coarse grids and conversely do not produce spurious distrubances, which is common with finite-difference and other numerical methods. However, the computed flow field for the coarser grid will have a truncation error for the larger grid spacing, and the flow field for the finer grid may also reflect this truncation error. For example, if a shock or contact surface travels from a fine grid into a coarse grid, then their locations become known less accurately (within one cell width of the coarser grid). On the other hand, when they travel from a coarse grid into a fine

grid their locations are now resolved to within one cell width of the finer grid, but they will be accurate only to within one cell width of the coarser grid because they originated in this coarser grid. Numerical experiments were also undertaken with rarefaction waves moving from fine to coarse grids and conversely, and no spurious disturbances were discovered.

6. Some Numerical Results

The advantage of using different node spacings in various parts of the numerical grid and local time stepping is the desirable reduction in computational time and cost. Such reductions may be highly significant, as will be demonstrated with examples herein.

Consider an explosion of a sphere of pressurized air in the atmosphere, for which the high-pressure air is initially at a uniform pressure and zero velocity. Let the sphere radius be 1.2 m, and let the numerical computations proceed until the shock reaches a radius of 7 m. Hence, the grid extends from 0 to 7 m. If an accurate computation of the flow properties inside a radius of 2 m is required, where flow properties may change markedly and have large gradients, then a large number of nodes such as 100 per meter may be required. If the node spacing was constant throughout the grid, then the total number of nodes would be quite large at 701. With this uniform node spacing the RCM would have to do 700 Riemann problems, 700 sampling assingments, and 700 time splitting corrections for the area changes per time step.

Such a RCM computer run was performed, for the case of a pressure ratio across the diaphragm of 7, and some of the numerical results are depicted in Fig. 9a. These pressure distributions with radius cover a total time period of 15 ms (every 0.833 ms). They are by and large very smooth, except nearer the origin where the operator-splitting corrections become larger, inaccurate, and thereby introduce more numerical noise. This noise may be reduced at any given radius, of course, by using more nodes. The CPU time for a minicomputer was 16.6 min.

The computational time may be reduced by using variable node spacing. Let the first meter contain 100 nodes as used previously, because a fine grid is required to resolve the steep gradients near the origin. Let the next two meters have 50 nodes each, where the gradients are less steep, and let the last four meters have 25 nodes each, where the flow properties vary rather smoothly (except at shocks and contact surfaces). The node spacing is now in the proportion of 1:2:4, and the total number of nodes has been reduced from 701 to 301. An unrefined RCM program would then solve 300 Riemann problems per time level, and also do 300 sampling assignments and time-splitting corrections per level, in order to achieve a savings in computational time and cost by a factor of about 7/3 or 2.33. (The time steps are essentially the same in both cases because the CFL time step prediction will be controlled by the smallest node spacing.)

This RCM computer run was done, and the numerical results are shown in

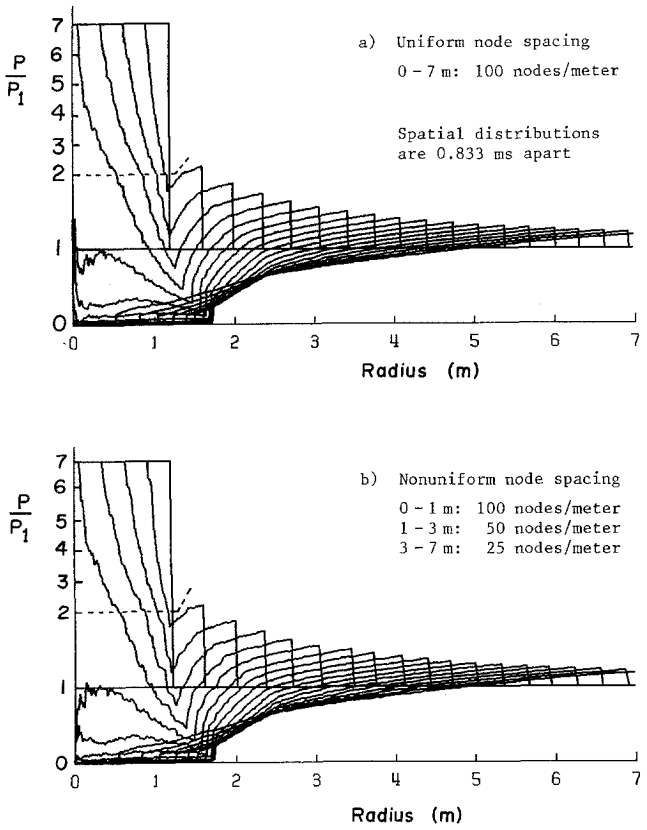

FIG. 9. Pressure distributions for the explosion of a 2.4-m-diameter sphere of air at an initial pressure ration of 7, computed with a uniform (a) and nonuniform (b) node spacing.

Fig. 9b for comparison directly to the last case. The two sets of results are for all practical purposes essentially the same, albeit there are some small differences. The pressure distributions at larger radii are not as smooth (having slightly larger undulations or noise), reflecting the slightly larger computational errors from a coarser node spacing. The outward moving shock also appears to have a less steep front farther from the origin, because it is plotted very simply as a linear change between the coarser adjacent nodes. With only 301 instead of 701 nodes, this computer run took only 7.6 min, for an overall decrease in computational time by a factor of 2.2. This is slightly lower than $\frac{7}{3}$ or 2.33 because some of the computer overhead remains identical for both runs.

Additional savings are still possible by using local time stepping. In terms of the present explosion problem, needless Riemann problems and sample assignements may be skipped when the random number Ω lies between $\frac{1}{4}$ and $\frac{1}{2}$ for the coarser node spacing of $2\,\Delta x_{\min}$ and when Ω lies between $\frac{1}{8}$ and $\frac{7}{8}$ for the even coarser node

spacing of $4\,\Delta x_{\min}$. In other words, the average number of useful Riemann problems with sample assignements per time level is 100 for the first zone with 100 nodes (0 to 1 m), 50 for the next zone with 100 nodes (1 to 3 m), and 25 for the last zone with 100 nodes (3 to 7 m), totalling on average only 175. As compared to the first case of 700 nodes, this would lead to a significant savings in computational time and cost by a factor of 4. However, when this was implemented in the computer program, the saving was slightly less at 3.6, because a few additional program statements are needed, some of the computer overhead remains the same for both runs, and operator-splitting corrections were not skipped. As one might expect, the numerical results were virtually identical to those already given in Fig. 9b for the case of variable node spacing. Hence, they are not shown here.

This savings factor of 3.6 for local time stepping should now be compared to the second computer run with a savings factor of only 2.2. By eliminating the needless Riemann problems and sample assignments, the savings in computational time has been increased by another significant factor of 1.7, without any reduction in the quality of the numerical results.

To further illustrate the computational savings made possible by using a nonstaggered grid with variable node spacing, one more problem is briefly mentioned. This is the case of a constant-area shock tube which is converted into a blast-wave simulator by inserting a set of five perforated plates in the driver [12], in order to control the mass flow out of the driver into the channel to produce therein a shock wave with a decaying signature. Each fairly thin perforated plate of 2 cm requires at least 10 nodes to represent the flow properties accurately, illustrating that 500 nodes per meter are necessary. Without using a variable node spacing the grid would require 4501 nodes for a shock tube that is 9 m long. With variable node spacing this may be reduced substantially as follows. At 500 nodes per meter there are 50 nodes in five perforated plates, taking up 10 cm of a driver that is 1 m long. If 200 nodes per meter are used in the remainder of the driver this results in 180 nodes. At 60 nodes per meter in the channel, which is 8 m long, the number of nodes is 481. Therefore, the 4501 nodes may be reduced to only 711 nodes, for a variable node spacing in the practical proportion of 1:2.5:8.33. Furthermore, by eliminating needless computations the average number of cells that actually need to be computed per time level would be decreased to only 180 (given by $50 + 180/2.5 + 480/8.33$), which is a highly significant reduction from 4500, and also from 710.

7. Discussion and Conclusions

The merits of using a nonstaggered grid instead of a staggered one are basically threefold. The first advantage is that the "housekeeping" or logic required in computer programs for the case of a nonstaggered grid is reduced, and this is especially true when variable node spacing is employed. The second advantage of employing a

nonstaggered grid in unrefined RCM computer programs is the reduction by a factor of about two in the storage requirements during computations, because values of the state and other variables are now needed at only about one-half the number of nodes. More refined computer codes that employ staggered grids can and have been programmed to reduce storage requirements [7–8, 12]; however, the additional effort with more complex program logic is now unnecessary. The last advantage is the ease in which local time stepping can be implemented in the case of nonstaggered grids with variable node spacing.

The implementation of variable grids and local time stepping has been introduced, and the significant saving in computational effort which can result has been demonstrated.

The most significant advantages of employing a nonstaggered grid with variable node spacing and local time stepping will apply in the solution of problems with more independent variables, such as two-dimensional unsteady flows. The use of the old staggered grid in such problems is particularly cumbersome in computer program logic and wasteful of computer storage. Although the RCM has not been very successful in solving such problems [3, 19], it is anticipated that this will change in the future.

ACKNOWLEDGMENTS

The author thanks Dr. E. F. Toro of the College of Aeronautics, Cranfield Institute of Technology, England, and Mr. C. P. T. Groth of the Institute for Aerospace Studies, University of Toronto, Canada, for useful discussions. This work was supported by the Natural Sciences and Engineering Research Council and Defince Research Establishment Valcartier, Courcelette, Quebec, both of Canada.

REFERENCES

1. S. K. GODUNOV, *Mat. Sb.* **47**, 271 (1959).
2. J. GLIMM, *Commun. Pure Appl. Math.* **18**, 697 (1965).
3. A. J. CHORIN, *J. Comput. Phys.* **22**, 517 (1976).
4. A. J. CHORIN, *J. Comput. Phys.* **25**, 253 (1977).
5. G. A. SOD. *J. Fluid. Mech.* **83**, 785 (1977).
6. P. COLELLA, *SIAM J. Sci. Stat. Comput.* **3**, 76 (1982).
7. T. SAITO AND I. I. GLASS, *Prog. Aerospace Sci.* **21**, 201 (1984).
8. G. A. SOD, *J. Comput. Phys.* **27**, 1 (1978).
9. J. J. GOTTLIEB AND O. IGRA, *J. Fluid Mech.* **137**, 283 (1983).
10. O. IGRA AND J. J. GOTTLIEB, *AIAA J.* **23**, 1014 (1985).
11. H. HONMA AND I. I. GLASS, *Proc. R. Soc. London A* **391**, 55 (1984).
12. K. Y. ZHANG AND J. J. GOTTLIEB, University of Toronto UTIAS Report No. 304, 1986 (unpublished).
13. G. MARSHALL AND B. PLOHR, *J. Comput. Phys.* **56**, 410 (1984).
14. Z. C. SHI AND J. J. GOTTLIEB, University of Toronto UTIAS Report No. 297, 1986 (unpublished).
15. Y. TAKANO, *J. Comput. Phys.* **67**, 173 (1986).

16. J. GLIMM, G. MARSHALL, AND G. PLOHR, *Adv. Appl. Math.* **5**, 1 (1984).
17. H. M. GLAZ AND T.-P. LIU, *Adv. Appl. Math.* **5**, 111 (1984).
18. Y. A. SHREIDER, *The Monte Carlo Method* (Pergamon, Oxford, 1966), Chaps. 1–2.
19. J. M. HAMMERSLEY AND D. C. HANDSCOMB, *Monte Carlo Methods* (Methuen, London, 1975), Chaps. 2–3.
20. J. G. VAN DER CORPUT, *Proc. K. Ned. Akad. Wet.* **38**, 813, 1058 (1935).
21. M. HOLT, *Numerical Methods in Fluid Dynamics* (Springer-Verlag, Berlin, 1984), p. 56.
22. H. OLIVIER AND H. GRONIG, *J. Comput. Phys.* **63**, 85 (1986).